Chapter 6
Fluidized-Bed Scaling

Abstract The principles on which the performance of a full-scale fluidized-bed reactor may be inferred from that of a cold, scaled-down model are outlined and lead to a review of the scaling rules developed in the recent past. Dimensional analysis based on the Buckingham π-theorem is described as well as the alternative approach based on the governing equations of conservation of mass and momentum of fluidized particles. Examples are given of both rigorous and simplified sets of dimensionless groups appropriate to the scaling process and a description is given of the way they are applied to bubbling beds. This is followed by a consideration of the scaling relationships relevant to circulating fluidized-bed combustors where additional groups such as the Damköhler numbers can be applied. Work on the validation of the scaling rules is then described and leads to a section in which scaling is analysed in terms of the non-linear chaotic behaviour of fluidized beds. The chapter ends with a description of the application of the scaling rules to a scaled-down model of a thermal denitration reactor and its internal structure as revealed by X-ray analysis.

6.1 Introduction

The development of a new process centred on a fluidized-bed reactor proceeds through a number of stages. Experiments on a laboratory bench-scale unit provide basic information concerning reaction kinetics, catalyst activity and deactivation, particle attrition and agglomeration etc. This stage would typically be followed by work on larger scale pilot and demonstration units proceeding eventually to the full-scale plant. In the early stages of development a decision would be made regarding the type of fluidized bed to be used: bubbling, turbulent, circulating, entrained flow etc. and information would be needed on the expected hydrodynamic behaviour of the chosen system. It would be desirable to be able to infer the behaviour of the full-scale unit from that of, say, the laboratory unit or the pilot plant i.e. to be able to scale up the hydrodynamics from the smaller to the bigger bed. In practice this is far from straightforward since large beds have different solids

J.G. Yates and P. Lettieri, *Fluidized-Bed Reactors: Processes and Operating Conditions*, Particle Technology Series 26,
DOI 10.1007/978-3-319-39593-7_6

circulation and gas-solid contacting patterns from smaller beds and a unit that performs well at pilot scale often falls short of expectation in the full-scale plant (Fitzgerald et al. 1984). To address this issue much work has been reported on efforts to develop criteria for hydrodynamic similarity between fluidized beds of different scales, temperatures and pressures and to identify the relevant parameters and variables necessary to achieve dynamic similarity. To this end it is necessary to match certain dimensionless groups that must be kept equal at all scales, a procedure traditionally used in other areas of engineering such as aircraft and ship design where wind tunnels and flow tanks are used to explore fluid flows, drag forces, pressure profiles etc. around small-scale models. To identify the relevant scaling parameters for fluidized beds dimensional analysis may be applied via the Buckingham π-theorem or by analysis of the governing differential equations and boundary conditions that completely define the system under consideration. A prerequisite of any such analysis is that the units to be matched by hydrodynamics must be geometrically similar i.e. they must be the same shape and all their linear dimensions must be related by a constant scale factor.

6.2 Dimensional Analysis

An early method is based on the Buckingham π-theorem. This states that the n independent parameters defining any physical system may be reduced to (n-k) dimensionless groups where k is the number of dimensionally independent parameters whose value is less than or equal to the number of dimensions (mass (M), length (L) and time (T)) in the original defining n parameters. Glicksman et al. (1994) demonstrated the use of the theorem to determine the dimensionless groups that govern the hydrodynamic behaviour of fluidized beds. Expressing the pressure drop through a bed, ΔP, as the dependent parameter in terms of the main independent parameters:

$$\Delta P = f(u_0, g, D, L, d_p, \rho_s, \rho_f, \mu, \phi) \tag{6.1}$$

where:

Symbol	Definition	Dimensions
u_0	superficial velocity	L/T
g	acceleration due to gravity	L/T^2
D	bed diameter	L
L	bed height	L
d_p	particle diameter	L
ρ_s	solids density	M/L^3
ρ_f	fluid density	M/L^3

(continued)

(continued)

Symbol	Definition	Dimensions
μ	fluid viscosity	M/(LT)
ϕ	particle sphericity	–

Choosing u_0, D and ρ_f as the dimensionally independent parameters and using these to non-dimensionalize the remainder leads to the following set of parameters that define the system:

$$\frac{\Delta P}{\rho_f u_0^2} = f\left(\frac{gD}{u_0^2}, \frac{L}{D}, \frac{d_p}{D}, \frac{\rho_s}{\rho_f}, \frac{\mu}{\rho_f u_0 D}, \phi\right) \tag{6.2}$$

As noted by Rüdisüli et al. (2012) however the π-theorem does not indicate whether the chosen list of independent parameters is complete, a problem not found with the alternative approach based on the governing equations of conservation of mass and momentum of fluidized particles. Several groups have explored this area (Horio et al. 1986; Zhang and Yang 1987; Foscolo et al. 1990; Chan and Louge 1992) but the most comprehensive investigations are those of Glicksman's group at MIT summarised by Glicksman et al. (1994) and Glicksman (2003). On the basis of the conservation equations of Anderson and Jackson (1967) they derived a so-called "full" set of dimensionless parameters as follows:

$$\frac{\rho_f \rho_s d_p^3 g}{\mu^2}, \frac{\rho_s}{\rho_f}, \frac{u_0^2}{gD}, \frac{\rho_f u_0 D}{\mu}, \frac{G_s}{\rho_s u_0}, \phi \tag{6.3}$$

For similarity it is also necessary to match the particle size distribution of the fluidized materials in both systems. In (6.3) the first term is the Archimedes number Ar (the ratio of gravitational to viscous forces), the third term is the Froude number Fr (the ratio of inertial to gravitational forces), the fourth is the Reynolds number Re_p(the ratio of inertial to viscous forces) and the fifth is the dimensionless solids circulation flux where G_s is the solids mass flux (kg/m^{2}s); this latter term is only of relevance for circulating beds.

Calculation of the operating conditions and parameter values for a large-scale bubbling-bed combustor and a small-scale cold model using air at standard conditions and based on (6.3) have been set out by Fitzgerald et al. (1984) and by Glicksman et al. (1994) as follows.

The gas/solid density ratios for the model (subscript m) and the combustor (subscript c) are matched as:

$$\left(\frac{\rho_f}{\rho_s}\right)_m = \left(\frac{\rho_f}{\rho_s}\right)_c \tag{6.4}$$

The Reynolds number and Froude number may be combined to give:

$$\frac{\rho_f u_0 D}{\mu}\frac{(gD)^{\frac{1}{2}}}{u_0} = \left(\frac{D^{\frac{3}{2}}}{v}g^{\frac{1}{2}}\right)_m = \left(\frac{D^{\frac{3}{2}}}{v}g^{\frac{1}{2}}\right)_c \tag{6.5}$$

where v is the kinematic viscosity of the fluidizing gas. From (6.5):

$$\left(\frac{D_m}{D_c}\right) = \left(\frac{v_m}{v_c}\right)^{\frac{2}{3}} \tag{6.6}$$

It is further shown that:

$$\left(\frac{D}{d_p}\right)_m = \left(\frac{D}{d_p}\right)_c \tag{6.7}$$

and:

$$\frac{u_{0m}}{u_{0c}} = \left(\frac{v_m}{v_c}\right)^{\frac{1}{3}} = \left(\frac{D_m}{D_c}\right)^{\frac{1}{2}} \tag{6.8}$$

Satisfying (6.6) and (6.8) the Reynolds and Froude numbers are kept identical.

Based on these relationships a comparison between a hot combustor and a cold model is shown in Table 6.1 while the relevant values for a pressurised combustor are shown in Table 6.2. In the latter case the two units are comparable in size but a reduction in model dimensions could be achieved by use of a gas of higher density than air such as a Freon.

As this shows in practice it is sometimes difficult to match all the groups between a large hot reactor such as a combustor and a cold model of

Table 6.1 Atmospheric combustor modelled by a bed fluidized with air at ambient conditions (Glicksman et al. 1994)

Given	Commercial bed	Scale model
Temperature (°C)	850	25
Gas viscosity (10^{-5} kg/ms)	4.45	1.81
Density (kg/m^3)	0.314	1.20
Derived from scaling laws		
Solid density	ρ_{sc}	$3.82\rho_{sc}$
Bed diameter, length etc.	D_c	$0.225D_c$
Particle diameter	d_{pc}	$0.225d_{pc}$
Superficial velocity	u_{0c}	$0.47u_{0c}$
Volumetric solid flux	$(G_s/\rho_s)_c$	$0.47(G_s/\rho_s)_c$
Time	t_c	$0.47t_c$
Frequency	f_c	$2.13f_c$

Table 6.2 Pressurized combustor modelled by a bed fluidized with air at ambient conditions (Glicksman et al. 1994)

Given	Commercial bed	Scale model
Temperature (°C)	850	25
Gas viscosity (10^{-5} kg/ms	4.45	1.81
Density (kg/m^3)	3.14	1.20
Pressure (bar)	10	1
Derived from scaling laws		
Solid density	ρ_{sc}	$0.382\rho_{sc}$
Bed diameter, length etc	D_c	$1.05D_c$
Particle diameter	d_{pc}	$1.05d_{pc}$
Superficial velocity	u_{0c}	$1.01u_{0c}$
Volumetric solid flux	$(G_s/\rho_s)_c$	$1.01(G_s/\rho_s)_c$
Time	t_c	$1.01t_c$
Frequency	f_c	$0.98f_c$

laboratory-scale dimensions. Rüdisüli et al. (2012) cite the example of a hot reactor 1.60 m in diameter operated at 320 °C and 2.5 bar pressure. To scale this unit with a cold model fluidized by air at ambient conditions requires a bed of 1.48 m diameter. Scaling down to 0.2 m diameter would require the use of particles of density 23,000 kg/m^3 operated at a pressure of 20 bar. To overcome this problem Glicksman et al. (1993) sought to relax some of the criteria on which the full set of scaling groups were based and so to reduce the number required for similarity. This was achieved by modifying the form of the fluid- and particle-phase stress tensors in the basic equations of motion at the viscous and inertial limits represented by the Ergun equation (6.9). This expresses the pressure drop, ΔP, through a bed of particles with a voidage ε as:

$$\frac{\Delta P}{L} = \frac{150(1-\varepsilon)^2}{\varepsilon^3}\frac{\mu u_0}{(\emptyset d_p)^2} + \frac{1.75(1-\varepsilon)}{\varepsilon^3}\frac{\rho_f u_0^2}{\emptyset d_p} \tag{6.9}$$

The first term on the right-hand side represents the pressure loss due to viscous effects while the second term accounts for the effects of inertia. For flow through fine particles at low Reynolds numbers ($Re_p < 4$) the viscous term dominates while for large particles and high Reynolds numbers ($Re_p > 1000$) the inertial term is dominant. For the viscous limit the governing parameters were shown to be:

$$\frac{\rho_s u_0 d_p^2}{\mu D}, \frac{gD}{u_0^2}, \frac{D}{L}, \phi \tag{6.10}$$

The product of the first and second terms was shown (Glicksman 1988) to be equivalent to the ratio of the superficial velocity, u_0, and the minimum fluidization

velocity, u_{mf}, thereby removing dependence on the Archimedes number and making the governing list:

$$\frac{u_{mf}}{u_0}, \frac{gD}{u_0^2}, \frac{D}{L}, \phi \tag{6.11}$$

In the inertial limit the governing list is:

$$\frac{gD}{u_0^2}, \frac{\rho_f}{\rho_s}, \frac{d_p}{D}, \frac{L}{D}, \phi \tag{6.12}$$

Glicksman et al. (1994) then combined (6.11) and (6.12) to give a set of parameters approximately valid for the intermediate region:

$$\frac{u_{mf}}{u_0}, \frac{gD}{u_0^2}, \frac{\rho_f}{\rho_s}, \frac{L}{D}, \phi \tag{6.13}$$

The advantage of the simplified set of scaling parameters is that they allow greater flexibility in the choice of dimensions of the small-scale unit removing the need for "exotic" particles and pressures (Rüdisüli et al. (2012).

Nicastro and Glicksman (1984) tested experimentally the full set of scaling parameters (6.3) by comparing the performance of a 0.61 m^2 and 4.4 m tall fluidized-bed combustor operated at 780 °C with a quarter-scale cold model. The operating conditions of the two beds are shown in Table 6.3 from which it may be seen that there is good agreement for all parameters except the density ratio as a result of the density of the iron powder being somewhat too low.

The similarity between the beds was tested by comparing pressure signals measured at different locations in the two beds. Figure 6.1 shows the power spectral

Table 6.3 Operating conditions in a coal-burning combustor and cold scale models fluidized with air (Nicastro and Glicksman 1984)

Bed material	Hot bed	Cold bed	Cold bed
	Sand and coal	Iron grit	Sand and coal
T_b (K)	1098	300	299
ρ_s (kg/m^3)	2630	7380	2630
d_p (μm)	677	170	677
u_0 (m/s)	0.93	0.47	0.94
L_f (m)	0.92	0.24	0.23
ε_{mf}	0.49	0.57	0.49
ε_f	0.60	0.64	0.62
u_{mf}	0.16	0.10	0.18
Re_p	5.17	5.33	41.8
Fr	129	130	132
ρ_s/ρ_f	7280	5920	2170
L_f/d_p	1360	1410	330
L/L_f	0.66	0.64	0.67

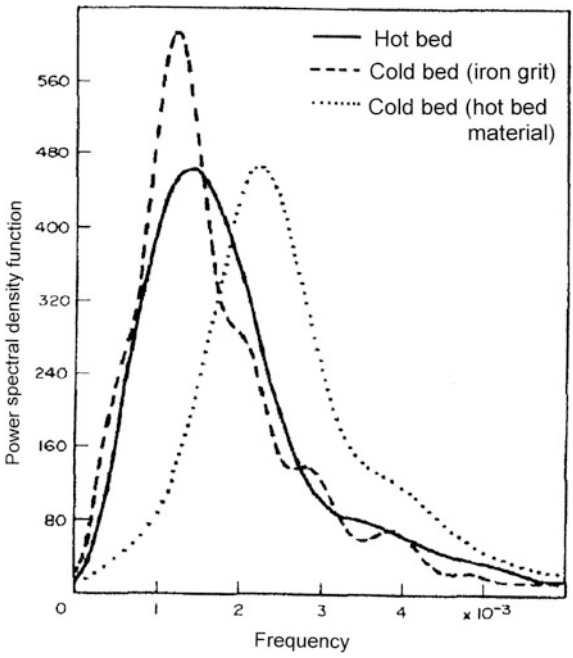

Fig. 6.1 Comparison of dimensionless power spectra of differential pressure fluctuations (Nicastro and Glicksman 1984)

density function and frequency measured by a probe situated at the wall. The plot shows good agreement between the hot bed and the cold bed containing iron powder but little agreement between the hot bed and the cold sand-containing bed indicating that modelling with identical bed material in a geometrically similar cold unit does not give dynamic similarity.

Roy and Davidson (1988) also used pressure measurements to compare bubbling beds at different temperatures and pressures—identities of dimensionless frequency and amplitude of pressure fluctuations indicating similarity. Their results showed that in the viscous limit at $Re_p < 30$ the reduced set of parameters given in 6.5/6.6 is sufficient to ensure dynamic similarity but that the full set (6.3) is necessary at $Re_p > 30$.

A number of other authors have developed scaling parameters for bubbling beds based on principles similar to or different from the above. Fitzgerald et al. (1984) also used the analysis of Anderson and Jackson (1967) to derive four dimensionless groups for similarity: the Froude number, the particle Reynolds number, the gas-to-solid density ratio and the ratio of a characteristic bed dimension to the average particle size. They used pressure fluctuation measurements to compare four different beds one of which was a 1.83 m^2 atmospheric combustor and another 0.46 m^2 cold bed of copper particles fluidized with air; autocorrelation plots of the pressure fluctuations for the two were found to be of the correct scaled frequency. Based on phenomenological models of bubble splitting and coalescence Horio et al. (1986) derived two scaling parameters:

$$\frac{u_0 - u_{mf}}{(gD)^{1/2}}, \frac{u_{mf}}{(gD)^{1/2}} \tag{6.14}$$

which were shown by Glicksman (1988) to be equivalent to those in (6.11) and thus to be only valid at the viscous limit. In a subsequent development by Horio et al. (1989) scaling relationships for circulating fluidized beds were obtained based on a model that assumes the riser of a CFB to have a core/annular structure with clusters of particles moving upwards in the core region and downwards in the annular region at the walls. Scaling was based on the equality of voidage distribution, dimensionless core radius, gas and solids splitting between core and annulus and cluster voidage. The similarity rules were tested experimentally using two geometrically similar scaled models (1/25 and 1/100) of a 175 MW CFB combustor. Axial voidage distribution, its transition and the radial distribution of cluster velocity in the scaled units were found to be in good agreement with those in the full-scale unit showing the validity of the proposed scaling law. Chang and Louge (1992) also considered scaling relationships for circulating fluidized beds on the basis of the continuum equations referred to above, deriving five dimensionless groups for flow of spherical particles in risers similar to those given in (6.3). For non-spherical materials however they followed the Ergun equation in combining the sphericity, ϕ, with the particle diameter, d_p, to produce the following:

$$\frac{\rho_f \rho_s \left(d_p \phi^{\alpha} g\right)^3}{\mu^2}, \frac{\rho_s}{\rho_f}, \frac{u_0}{\left(g d_p \phi^{\alpha}\right)^{\frac{1}{2}}}, \frac{D}{d_p \phi^{\alpha}}, \frac{G_s}{\rho_s u_0} \tag{6.15}$$

Here d_p is the diameter of a sphere having the same volume as the non-spherical particle, α is an empirical constant and D is the diameter of the riser. Experimental tests were carried out with three risers 0.32, 0.46 and 1 m in diameter with plastic, glass and steel powders, static pressures and pressure fluctuations being used to test for dynamic similarity. The results showed that in risers of moderate diameter vertical pressure profiles scale with riser diameter and particle density whereas pressure fluctuations scale with the product of particle diameter, density and sphericity.

On the basis of the one-dimensional "particle-bed model" Foscolo et al. (1990) derived a further set of scaling parameters:

$$\frac{g d_p^3 \rho_f^2}{\mu^2}, \frac{\rho_f}{\rho_s}, \frac{u_0}{u_t} \tag{6.16}$$

where u_t is the terminal-fall velocity of a single particle. They used these to compare the observed behaviour of a number of fluidized systems comprising different solids and fluids e.g. alumina—high pressure CF_4 gas (Crowther and Whitehead 1978), copper-water (Gibilaro et al. 1986), carbon-synthesis gas (Jacob and Weimer 1987). The object was to compare the bed voidage, ε_{mb}, at the point of transition from homogeneous to bubbling fluidization. Thus a copper-water system

was matched to a carbon-high pressure gas (124 bar) system when both showed closely similar ε_{mb} values of 0.66 and 0.68 respectively. A system of soda-glass particles fluidized with water was matched with one of alumina particles fluidized by high-pressure gas: both, as predicted by the model, showing stable homogeneous behaviour throughout the range of velocities investigated (Gibilaro 2001).

6.3 Combustion Scaling

Leckner et al. (2011) reviewed work on the scale-up of circulating fluidized-bed combustors and described research carried out at Chalmers University with a 12 MW boiler and a 1/9th scale plastic model operated at ambient conditions. The boiler was operated with sand and low-ash wood chips while the scaled unit used iron and steel particles whose densities and shapes deviated somewhat from the required values indicated by the scaling set (6.3). The authors emphasised the fundamental difficulty in dynamic scaling of finding particles of the correct size, shape and density for the cold model. Experimental results in the case of the iron particles showed good correspondence between the solids volume fraction along the height of the riser in both model and boiler; correspondence in the case of the steel particles was not so good and was unexplained. Good agreement between gas-dispersion measurements was found for both materials as shown in Fig. 6.2.

The authors then discussed the question of combustion scaling as opposed to hydrodynamic scaling. In the former case combustion usually takes place in both the small and large plants and for scaling purposes a number of parameters may be

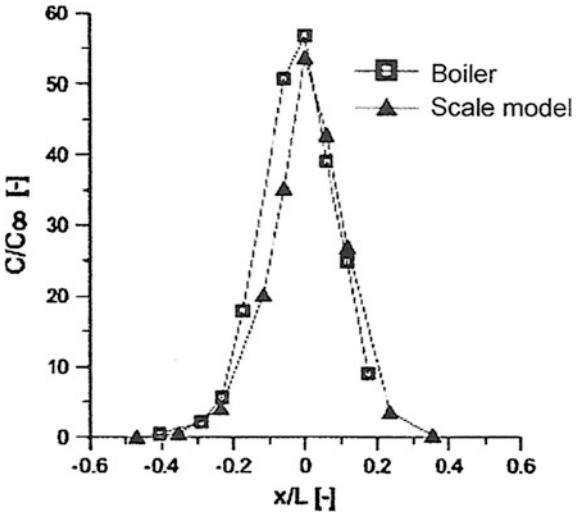

Fig. 6.2 Gas-concentration profiles from tracer-gas injection in the boiler and scale model (Leckner et al. 2011)

maintained identical in a test plant and a full-scale boiler. Such parameters are bed temperature, total excess-air ratio, primary-air stoichiometry, fuel and bed material. The fluidization-gas velocity should also be kept to the same order of magnitude in the two plants. Scaling then requires determination of the linear dimensions (height, L, and diameter, D) of the test riser as well as that of the solids mass flux. In general it is only feasible to apply scaling criteria to the riser of a CFB boiler since in a small-scale unit, although the riser height may be of comparable size, the diameter must be kept small; normally L/D > 30 in the model and L/D < 10 in the boiler. Leckner et al. (2011) firstly considered the horizontal-scaling problem related to the transport of fuel particles from distribution points at or near the wall of a riser. They cited the earlier work of Leckner and Werther (2000) who proposed the Damköhler number *Da* (ratio of transport time to reaction time) as a criterion for combustion scaling. Values of *Da* were determined on the basis of the two processes occurring when fuel is introduced into a combustor namely devolatilization and char combustion. The devolatilization/reaction time, t_v, for a particle of diameter d_p was taken as:

$$t_v = ad_p^2 \tag{6.17}$$

where a, an empirical constant, was given the value 10^6 s/m^2. Char combustion was assumed to be diffusion controlled giving the burn-out time, t_c, as:

$$t_c = \frac{\rho_c d_p^2}{48 Sh D_g c_0} \tag{6.18}$$

The average dispersion distance, x, was determined from an expression derived by Einstein (Gardiner 1997) for the dispersion time, t_d, in Brownian motion:

$$t_d = x^2/2D_h \tag{6.19}$$

where the horizontal dispersion coefficient, D_h, had a value 0.01 m^2/s. For high-volatile fuels reaction time was equated to devolatilization time and the horizontal Damköhler number, Da_h, results from combining (6.17) and (6.19) to give:

$$Da_h = \left(\frac{x}{d_p}\right)^2 \left(\frac{1}{2aD_h}\right) \tag{6.20}$$

$$= 50\left(\frac{x}{1000 d_p}\right)^2 \tag{6.21}$$

and hence $Da_h \leq 1$ for $(x/1000d_\mathrm{p}) \leq 0.14$. This result shows that for a 1 mm diameter high-volatile fuel reaction in the horizontal direction will be completed in risers of diameter 0.14 m or less and for a 10 mm diameter material 1.4 m or less. The consequence is that scale-up from a small to a larger unit will be unreliable

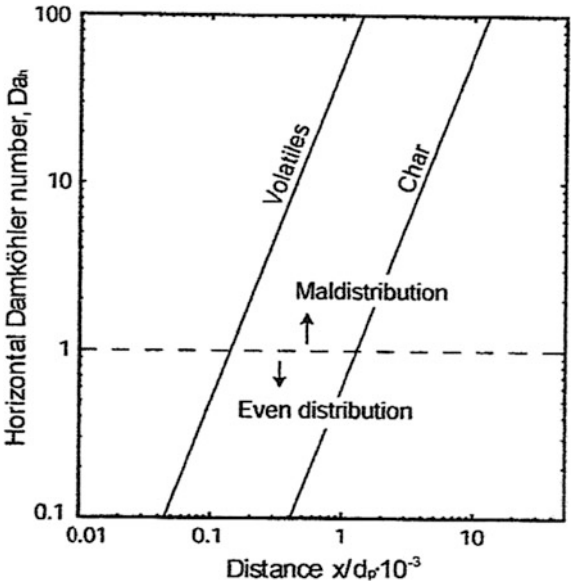

Fig. 6.3 Horizontal Damköhler number versus dimensionless dispersion distance (Leckner et al. 2011)

since maldistribution of fuel and air will be prevalent in a large plant but not in a small-scale unit where mixing will be more efficient. For char combustion Da_h is formed from (6.17) and (6.18) leading to $Da_h \leq 1$ for $(x/1000d_p \leq 1.4$ and so fuel dispersion should be at less than 1.4 m for a 1 mm char particle and scale-up should be reliable. These results are shown diagrammatically in Fig. 6.3 which indicates that devolatilization is much faster than char combustion and that Da_h depends on the size of the fuel particle: larger particles are transported further before undergoing reaction.

These conclusions were borne out by the report by Alliston and Wu (1996) on work with a small-scale combustor burning bituminous coal in a bed of limestone and a 5 m diameter combustor where the pilot plant always performed better in terms of sulphur capture than the larger bed. Mixing was less critical in the smaller bed where the fuel-air mixture was more homogeneous in the vicinity of the fuel injection point.

Scaling in the vertical direction of a riser was again a function of fuel-particle size and composition. If fuel-air mixing at the entry point is efficient volatiles combustion will be complete before particles exit to the cyclone. Char combustion however is slower and a fraction of the material $(1 - \eta)$ will leave the cyclone and need to be recirculated; here $(\eta < 1)$ is the cyclone collection efficiency. The time spent by char particles in the reactive environment of the riser of length L is then:

$$t_t = \frac{L/u_p}{(\eta - 1)} \tag{6.22}$$

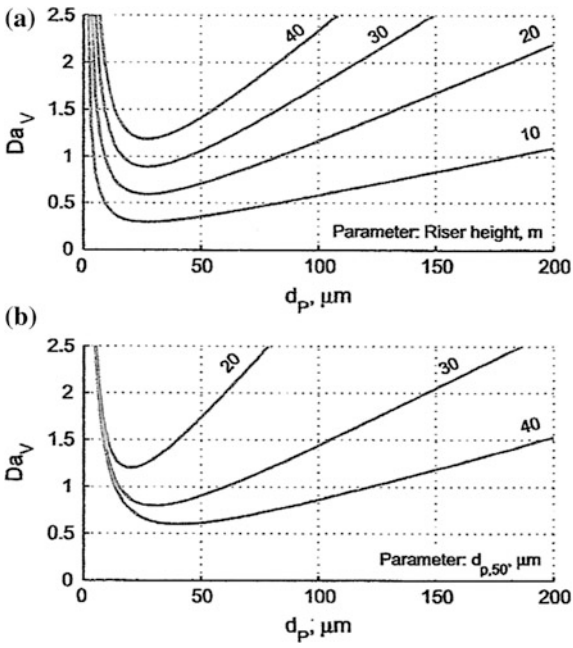

Fig. 6.4 Vertical Damköhler number versus char particle size (Leckner et al. 2011)

where $u_p = (u_0 - u_t)$, u_t being the terminal fall velocity of a single particle. The vertical Damköhler number is then:

$$Da_v = t_t / t_{char} \tag{6.23}$$

For vertical scaling Da_v should be greater than unity and as shown in Fig. 6.4a small particles will have sufficient time to react in their passage through tall risers; the influence of the cyclone efficiency on char burn-out is shown in Fig. 6.4b.

6.4 Validation of the Scaling Laws

Differential pressure fluctuations as measured by pressure probes immersed in the bed have frequently been used to test the validity of the scaling relationships. The fluctuations may be analysed statistically in terms of their spectral power density, as was demonstrated by Fitzgerald et al. (1984) and Nicastro and Glicksman (1984), or their probability density function as used by Sanderson and Rhodes (2005). In this latter study the simplified laws of Glicksman and Horio were tested with a set of four cylindrical cold model beds ranging in diameter from 146 to 1560 mm i.e. a ten-fold difference; the beds were operated at ambient temperature with spherical glass particles of various sizes fluidized with air. Pressure fluctuation measurements were made with probes situated at a number of locations distributed axially and

radially within the beds. Based on the statistics derived from these measurements the authors generated an "agreement map" showing the extent of agreement with the scaling parameters in various regions of the beds. Good agreement was found generally with the small-scale beds but with the largest bed at gas velocities up to 3.5 u_{mf} poor agreement was found at the walls and towards the bed surface.

Di Felice et al. (1992) studied the scale-up rules established earlier (6.16) using five different gas-solid systems fluidized with air at ambient temperature and at different pressures in the bubbling and slugging regimes. Three of the systems examined used spherical particles and were dynamically similar, one used non-spherical particles and one was deliberately mismatched; again pressure fluctuations were applied to test similarities. Good agreement was found for the dynamically similar systems in the bubbling regime but not when the beds were in operated in slugging mode. Poor agreement was found for the other two systems.

Chaos analysis

A fluidized bed can be considered to be a non-linear chaotic system in which the governing variables may be projected into a multi-dimensional state space represented by a so-called "attractor" which gives a characteristic fingerprint of the system (van Ommen et al. 1999). Beds showing similar attractors may be considered to have similar hydrodynamic properties whereas variations in one bed's attractor over time indicate changes in its hydrodynamics. Such changes with time have been used to detect particle agglomeration (van Ommen et al. 2000). It was shown by Takens (1981) that the attractor may be reconstructed from the time series of one characteristic variable such as the local pressure variation (Fig. 6.5) and to compute the attractor of a fluidized bed B_1 a series of instantaneous pressure measurements (p_1, p_2 ... p_N) is made.

The values are then normalised by subtracting their average value from each reading and dividing by the standard deviation to give a time series x_k with N values a mean of zero and a standard deviation of unity. A similar procedure is followed for a second bed B_2 to give a time series y_k. The pressure-time series x_k is then converted to a set of $(N - m + 1)$ delay vectors X_k with m elements which can be considered as points on an m-dimensional state space leading to the reconstructed attractor for B_1 denoted as $\rho_X(X_i)$. The attractor for B_2, $(\rho_Y(Y_i))$, is constructed in a

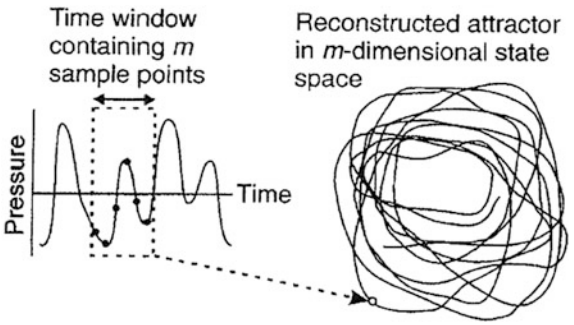

Fig. 6.5 Reconstruction of an attractor in the m-dimensional state space from a pressure-time series (van Ommen et al. 2000)

similar way and the extent to which the two attractors differ is given by the squared distance Q between them. An unbiased estimator Q' of this difference was calculated by Diks et al. (1996) and this along with the variance of the estimator V leads to a defining statistic S such that:

$$S = \frac{Q'}{\sqrt{V(Q')}} \tag{6.24}$$

If S is close to zero the two attractors and hence the two hydrodynamics are similar and the beds are correctly scaled; if $S > 3$ the two are different.

The attractor-comparison method was used by van Ommen et al. (2004) in an attempt to validate the scaling rules proposed by Horio et al. (1986). They found that while the original tools usually indicated similarity the statistical method showed disagreement. A similar conclusion was reached in a separate study by van Ommen et al. (2006). Pending further investigations the question remains open.

6.5 Application of the Scaling Laws to the Thermal Denitration Reactor at Sellafield, UK

In this section we present an example of the application of the scaling rules developed by Glicksman et al. (1994) applied to the design of a 4/10 scaled down model of the Magnox Reprocessing Thermal Denitration (TDN) fluidized-bed reactor operated at the nuclear fuel reprocessing site at Sellafield. This application is an example where employing in a laboratory scale model the fluids and the real solids as in the commercial process (and the reaction temperature), is impossible. Hence, in this case the scaling rules for fluidization are a fundamental tool to guide the design of a scale down system in which the fluid-dynamics of the real scale reactor may be replicated.

The Magnox reprocessing and uranium finishing plants have been at the heart of the UK's nuclear fuel reprocessing programme for over 50 years, reprocessing over 50,000 tonnes of irradiated uranium fuel from the UK's fleet of Magnox nuclear power stations. The Uranium Finishing Line, principally the Thermal Denitration Reactors (TDN's) convert uranyl nitrate (liquid) into uranium trioxide (a solid powder product) that can be manufactured into fuel and re-introduced into the nuclear fuel cycle. The TDN reactor is a fluidized-bed reactor, in which heated fluidizing air is introduced through nozzles at the base of the reactor to thermally de-nitrate the uranyl nitrate forming uranium trioxide. The aging MagnoxTDN reactors were becoming increasingly unreliable and restricted throughput of the reprocessing plant on many occasions. A major project was therefore initiated at UCL (Lettieri et al. 2014; Materazzi and Lettieri 2016) in collaboration with the National Nuclear Laboratory (NNL) and Sellafield Ltd. to investigate and resolve a number of operational problems occurring in the full scale TDN reactor at

Sellafield. The dimensionless parameters proposed by Glicksman et al. (1994) proved to be a reliable guide for the design of a 4/10 scale lab model operated under ambient conditions at UCL.

In this project, the unique X-ray imaging facility available at UCL (Lettieri and Yates 2013) was used to reveal for the first time the flow patterns inside such reactors and their fluidization performance (Holmes et al. 2015). X-ray studies of full scale sections of commercial units have been used to assess proposed process improvements, particularly in cases where there are significant internal hardware components such as cooling/heating coils, liquid spray nozzles, and feed gas spargers (Newton 2004). The advantage of X-raying a full scale section is that any uncertainties about the experimental conclusions are minimised even in cases where no reactions are taking place in the model reactor.

The process design followed to realize the 4/10 scaled-down TDN reactor is described: prior to the application of the scaling rules for fluidization, the geometry of the commercial reactor had to be scaled down. In this case a 4/10th scale was identified with NNL as being sufficiently large to avoid undesired interference from the reactor walls, whilst also allowing X-ray examination of the vessel. The complex reactor geometrical configuration of the real scale reactor and the hydrodynamic parameters were maintained in the scale down model to reproduce the fluidisation behaviour under ambient conditions. Hence, the geometric configuration for the bed, i.e. height-to-width ratio, internals (heating tubes) and distributor configuration was maintained, with the number of heater tubes being reduced according to the same 4/10 ratio. The comparison of reactor dimensions between the model and commercial scale is shown in Fig. 6.6.

The conical base section of the TDN reactor was the most complex part to model as it accommodates the central and upper air fluidization rings, as well as the ring to hold the internal heating tubes. A diagram of the lab scale conical section is shown in Fig. 6.7, where the 3 gas injection levels are shown schematically as shaded at levels 1, 3 and 5, whilst the dummy heating tubes (levels 2 and 4) are unshaded in the diagram. Although the geometrical characteristics of the conical base of the real TDN (see Fig. 6.8a) could not be replicated exactly in the scale down model (Fig. 6.8b), the design of the conical base was carefully devised so to obtain the required flow rates. Gas flow rates for the commercial scale and scale down reactors are shown in the Table 6.4.

Having matched the geometric scaling described above, the simplified Glicksman scaling laws allowed determination of the physical characteristics of the bed material and the operating conditions to be adopted so as to achieve fluid dynamically equivalent conditions in the scale down model compared to the full-scale system. Table 6.5 shows a comparison of the operating parameters used in TDN reactor, the values of the calculations for an exact match and the values which were selected to be as close as practicable.

A comparison of the reduced set of reaction parameters matched for hydrodynamic equivalence is shown in Table 6.6. The closest practical solid (to uranium trioxide powder) chosen for the study was (titanium oxide) sand which has a particle density of 4600 kg/m^3 and the desired particle size distribution and gave a

Scale:	10		4	
Dimensions:				
	Real size		Lab scale	
A	3.486	m	1.3944	m
B	1.216	m	0.4864	m
C	0.3	m	0.12	m
D	0.914	m	0.3656	m
E	1.42	m	0.568	m
F	0.76	m	0.304	m
G	4.223	m	1.6892	m

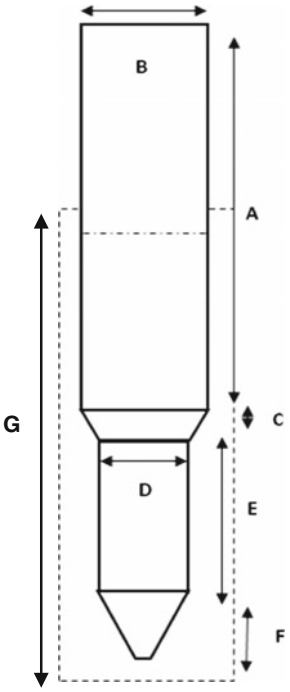

Fig. 6.6 Comparison of dimensions between commercial and lab scale reactor

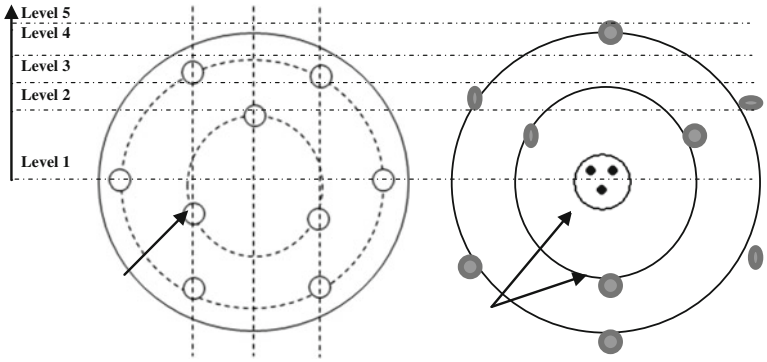

Fig. 6.7 Design of the conical section, comprising the aeration nozzles and the dummy heating pipes

satisfactory match to the 4800 kg/m^3 required by the simulation calculations. Titanium dioxide powder was used for the experiments, which was a close match to the material identified with the scaling rules and also matched the physical characteristics of the uranium trioxide (UO_3) produced in the TDN reactor at Sellafield. Figure 6.8 shows the final CAD design and the 4/10th scale TDN reactor which was designed and built at UCL.

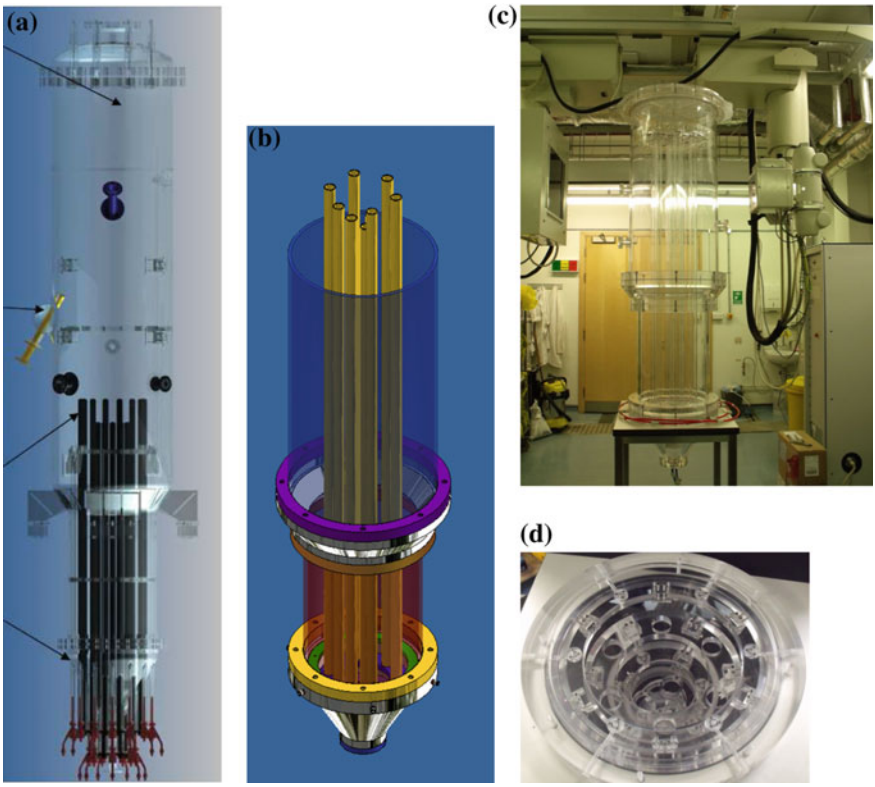

Fig. 6.8 **a** schematic of the TDN reactor at Sellafield; **b** CAD design of Lab Reactor alongside the Perspex Scale down TDN Modeling the X-ray Cell at UCL **c**; and **d** a detailed view of the conical section (refer also to Fig. 6.7)

Table 6.4 Gas flow rates for the commercial scale and scale down reactors

	Original TDN			Cold model		
	Central nozzle	Central ring	Upper ring	Central nozzle	Central ring	Upper ring
Number of air nozzles	7 (fissures)	7	14	3	3	6
Air rate (m^3/h)	90.00	135.00	270.00	10.33	15.5	31.00
Air flow through 1 nozzle (m^3/h)	13.00	19.28	19.28	3.44	5.16	5.16

Although with this particular application, experimental data from the full scale plant could not be provided to validate the application of the scaling rules, the experimental evidence (over 40,000 X-ray images taken) obtained with the 4/10th scaled down TDN model was successfully used to provide information on the jet penetration into the conical section of the TDN, the bubble dynamics evolving in

Table 6.5 Comparison of operating parameters

Parameter	TDN	Exact cold model	Actual cold model
T (C)	300	10	15
P (bar)	3	1	1
μ (kg/ms)	2.993E−05	1.78E−05	1.81E−05
ρ_g (kg/m3)	1.841	1.24	1.33
ρ_s (kg/m3)	7100	4800	4600
Φ	0.77	0.77	0.77
u_{mf} (m/s)	0.00817	0.00513	0.00457
u_o (m/s)	0.26	0.16	0.16
D (m)	0.914	0.3656	0.36
dp (μm)	100	63.1	60

Table 6.6 Simplified scaling parameter values

Scaling parameter	TDN	Cold model
ρ_s/ρ_g	3855.98	3461
u_0^2/gD	0.00756	0.00751
u_0/u_{mf}	31.85	32.01
Φ	0.77	0.77

the upper sections of the reactor, the bubble induced solids mixing and elutriation, and nozzles performance. Figure 6.9 shows some of the X-ray images obtained during this project.

Thanks to the application of the scaling rules for fluidization, extensive and systematic experiments were undertaken in the 4/10 scale TDN and several recommendations were made which led to the improvement of the solids mixing, heat transfer and reactor control of the real TDN. Sellafield Ltd., as a result of this project, has seen a massive improvement in operational reliability and throughput of the Magnox TDN Reactors—these are now no longer perceived as "high risk" to the operation of Magnox Reprocessing. The objectives of the NDA's UK Strategy for hazard reduction have been addressed and the risk of the possible requirement for alternative long term fuel storage for Magnox spent fuel has been mitigated, with potential substantial savings for the UK Taxpayer.

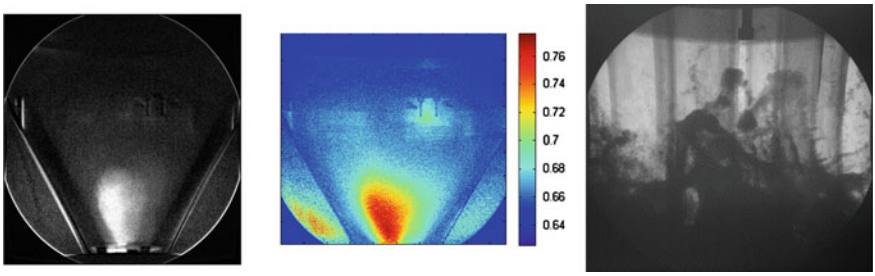

Fig. 6.9 (*left*) central nozzle jet into the conical section of the 4/10 scale TDN; (*centre*) voidage distribution around the central jet; (*right*) particle motion in the freeboard

References

Alliston MG, Wu S (1996) SO_2 distribution in large CFB combustors and its impact on sorbent requirements. CFB Technology. Science Press, Beijing, pp 327–332

Anderson TB, Jackson R (1967) A fluid-mechanical description of a fluidized bed. Ind Eng Chem Fundam 6:527–539

Chang H, Louge M (1992) Fluid dynamic similarity of circulating fluidized beds. Powder Technol 70:259–270

Crowther ME, Whitehead JC (1978) Fluidization of fine powders at elevated pressures. Fluidization. Cambridge University Press, Cambridge

Diks C, van Zwet WR, Takens F, de Goede J (1996) Detecting differences between delay vector distributions. Phys Rev E 53:2169

Di Felice R, Rapagna S, Foscolo PU (1992) Dynamic similarity rules: validity check for bubbling and slugging beds. Powder Tech 71:281

Fitzgerald T, Bushnell D, Crane S, Sheih Y-C (1984) Testing of cold scaled-bed modelling for fluidized-bed combustor. Powder Technol 38:107–120

Foscolo PU, Di Felice R, Gibilaro LG, Pistone L, Piccolo V (1990) Scaling relationships for fluidization: the generalised particle bed model. Chem Eng Sci 45:1647–1651

Gardiner CW (1997) Handbook of stochastic methods, 2nd edn. Springer, Berlin

Gibilaro LG, Hossain I, Foscolo PU (1986) Aggregate behaviour of liquid fluidized beds. Can J Chem Eng 64:931–938

Gibilaro LG (2001) Fluidization-dynamics. Butterworth Heinemann, Oxford

Glicksman LR (1988) Scaling relationships for fluidized beds. Chem Eng Sci 43:1419–1421

Glicksman LR. Hyre M, Woloshun K (1993) Simplified scaling relations for fluidized beds. Powder Technol 77:177–199

Glicksman LR, Hyre MR, Farrell PA (1994) Dynamic similarity in fluidization. Int J Multiph Flow 20:331–386

Glicksman LR (2003) Fluidized-bed scale-up. In: Yang W-C (ed) Handbook of fluidization and fluid-particle systems. Marcel Dekker, New York

Holmes R, Materazzi M, Gallagher B (2015) 3D printing and X-ray imaging applied to thermal denitration at Sellafield. Nucl Future J 12(6):33

Horio M, Nonaka A, Sawa Y (1986) A new similarity rule for fluidized-bed scale-up. AIChE J 32:1466–1482

Horio M, Ishii H, Kobukai Y, Yamanishi N (1989) A scaling law for circulating fluidized beds. J Chem Eng Jpn 22:587–592

Jacob KV, Weimer AW (1987) High temperature particulate expansion and minimum bubbling of fine carbon powders. AIChE J 33:1698–1706

Leckner B, Werther J (2000) Scale-up of circulating fluidized-bed combustion. Energy Fuels 14:1286–1292

Leckner B, Szentannai P, Winter F (2011) Scale-up of fluidized-bed combustion. A review. Fuel 90:2951–2964

Lettieri P (2014) Design, manufacture and X-ray Imaging of a scaled down TDN fluid bed reactor. Keynote, Particulate systems analysis conference, Manchester, 15–17 September

Lettieri P, Yates JG (2013) New Generation X-ray Imaging for multiphase systems. In: Fluidization XIV, Leeuwenhorst, Noordwijkerhout, The Netherlands

Materazzi M, Lettieri P, Holmes R, Gallagher B (2016) Magnox reprocessing TDN reactors: utilising 3D printing and X-ray imaging to re-design and test fluidising air nozzles. In: Proceedings of Waste Management, Phoenix, Arizona

Newton D (2004) Revealing the secrets of fluidized beds, exploiting links between academia and industry. Ingenia, (14):47–52

Nicastro MT, Glicksman LR (1984) Experimental verification of scaling relationships for fluidized beds. Chem Eng Sci 39:1381–1391

Roy R, Davidson JR (1988) Similarity between gas-fluidized beds at elevated temperature and pressure. Fluidization VI. Engineering Foundation, New York, pp 293–300

Rüdisüli M, Schildhauer TJ, Biollaz SMA, van Ommen JR (2012) Scale-up of bubbling fluidized-bed reactors: a review. Powder Technol 217:21–38

Sanderson J, Rhodes M (2005) Bubbling fluidized bed scaling laws: Evaluation at large scales. AIChE J 51:2686–2694

Takens F (1981) Detecting strange attractors in turbulence. In: Rand D, Young L-S (eds) Lecture notes in Mathematics vol 898, Dynamical systems and turbulence. Springer, Berlin

van Ommen JR, Schouten JC, Coppens M-O, van den Bleek (1999) Monitoring fluidization by dynamic pressure analysis. Chem Eng Technol 22:773–779

van Ommen JR, Coppens M-O, van den Bleek CM, Schouten JC (2000) Early warning of agglomeration in fluidized beds by attractor comparison. AIChE J 46:2183–2197

van Ommen JR, Sanderson J, Nijenhuis J, Rhodes MJ, van den Bleek CM (2004) Reliable validation of the simplified scaling rules for fluidized beds. Fluidization XI Engineering Conferences International, New York, pp 451–458

van Ommen JR, Teuling M, Nijenhuis J, van Wachem BGM (2006) Computational validation of the scaling rules for fluidized beds. Powder Technol 163:32–40

Zhang MC, Yang RYK (1987) On the scaling laws for bubbling gas-fluidized-bed dynamics. Powder Technol 51:159–165